A Low-cost Dopant additive free Hole Transporting Material for Robust Perovskite Solar Cell with Efficiency Exceeding 21%

Hongwei Zhu[†, ‡, §], Zhongjin Shen[,‡], Linfeng Pan[‖], Jianlei Han[†, §], Felix T. Eickemeyer[‡], Xianggao Li[*, †, §], Shirong Wang[†, §], Hongli Liu[†, §], Xiaofei Dong[†, §], Shaik M. Zakeeruddin[‡], Anders Hagfeldt[‖], Michael Grätzel[*, ‡] and Yuhang Liu[*, ‡]*

†Tianjin University, School of Chemical Engineering and Technology, Tianjin 300072, China;
‡Laboratory of Photonics and Interfaces (LPI), Department of Chemistry and Chemical Engineering, École Polytechnique Fédérale de Lausanne, Lausanne CH-1015, Switzerland.
§Collaborative Innovation Center of Chemical Science and Engineering, Tianjin 300072, China.
‖Laboratory of Photomolecular Science (LSPM), École Polytechnique Fédérale de Lausanne, Station 6, CH-1015 Lausanne, Switzerland.

Keywords: perovskite solar cells, hole transporting material, dopant additive free, high efficiency

Abstract

Developing hole-transporting materials (HTMs) with appropriate molecular configuration and charge mobility is important to improve perovskite solar cell (PSC) photovoltaic performance and their feasibility for commercialization. In this work, a novel pyramidal-shaped low-cost HTM coded MeOTTVT is prepared through extension of π-conjugation based on a triphenylamine core. Carbon-carbon double bonds are introduced between the core and *p*-methoxyl triphenylamine to improve the planarity of the HTM, favoring intermolecular stacking of MeOTTVT and thus improve the hole mobility of the corresponding hole transporting layer (HTL). Meanwhile, the *p*-methoxyl triphenylamine endowed HTM benefits from a well-aligned highest occupied molecular orbital (HOMO) level with the perovskite active layer, facilitating effective hole-extraction. Champion PSC using MeOTTVT-based dopant additive free HTL yielded power conversion efficiency (PCE) up to 21.30%, which is considered one of the best performing PSCs employing dopant additive free small molecule HTM. In addition, MeOTTVT-based dopant additive free HTL exhibits outstanding thermal stability and high glass-transition temperature (T_g =137.1 °C), combined with more hydrophobic surface, PSCs based on MeOTTVT dopant additive free HTL exhibits outstanding stability against moisture and thermal stress.

Introduction

Development in the last decade of perovskite solar cell (PSC) pushed the power conversion efficiency (PCE) from 3.8% to 25.2%[1-2]. With improved PCE, the research focus of PSCs has gradually shifted to commercialization, which is restricted mainly by the poor stability of PSCs resulting from hydrophilicity of the ionic perovskite active layer[3-6], which contrasts with the robustness of the transporting layers together with lowering production-cost[7-8]. Research efforts had been concentrated on optimization of the composition of the perovskite active layer[8-13] or increasing the surface hydrophobicity[14-16] to improve the stability of the PSCs. Hole transporting layer (HTL) is applied in the standard n-*i*-p architecture of PSC to selectively extract photo-generated holes and block electrons to avoid shunt[17-20]. 2,2',7,7'-tetrakis[N,N-di(4-methoxyphenyl)amino]-9,9'-spirobifluorene *(spiro*-OMeTAD) is one of the most widely used hole transporting material (HTM) yielding a PCE of corresponding PSCs of up to 24.66%[21]. However, it is normally considered that *spiro*-OMeTAD may not the best choice for practical application because of its high cost[22-24], tendency to crystallize at 85 °C and low intrinsic hole-mobility[25]. Chemical dopants such as Li-bis(trifluoromethanesulfonyl)-imide (Li-TFSI) and *tert*-butylpyridine (*t*BP) are introduced to *spiro*-OMeTAD based HTL as p-dopants, can affect the long-term stability of PSCs[26-28]. Li^+ movement has been witnessed during operational conditions where an internal electrical field is present[29]. Meanwhile, the doping process will also increase the complexity and cost of the PSCs fabrication[30]. Therefore, it is important to identify new low-cost HTMs exhibiting high hole-mobility and operational stability. Generally, dopant additive free HTMs include inorganic HTMs[31-32], polymer HTMs[33] and small organic HTMs[34-35]. Attentions have been drawn to the small organic HTMs because of the tunable molecular configuration, energy levels, and relatively low synthetic cost[36]. While previous studies reported dopant additive free small organic HTMs, such as TTE-2[37], DFH[38], Z1011[39], TPA-ANT-TPA[40] and MPA-BTTI[41] achieving PCEs up to 21.17%[41], it remains challenging to develop high performance dopant additive free HTMs with low-cost, to push further large spread applications of the PSC technology.

In this work, we report the design and synthesis of a novel small molecular HTM, MeOTTVT. The molecular structure of MeOTTVT is shown in **Figure 1a**. To obtain appropriate energy level, hole mobility and solubility, triphenylamine (TPA) with the quasi-3D pyramidal structure was selected as the core of MeOTTVT. Carbon-carbon double bonds were employed between TPA core and methoxy-substituted TPA arms to further enhance the molecular planarity, which is beneficial to improve hole mobility. Moreover, methoxylated-TPA arms can improve the contacts by forming a stable interface with the perovskite surface[42]. When fabricated into solar

cell, MeOTTVT dopant additive free HTL based PSC obtains a PCE up to 21.3% with a negligible hysteresis and exhibits good stability under thermal and humid conditions. Such a PCE is considered the best performing dopant additive free small molecule HTM based PSC so far (**Table S4**).

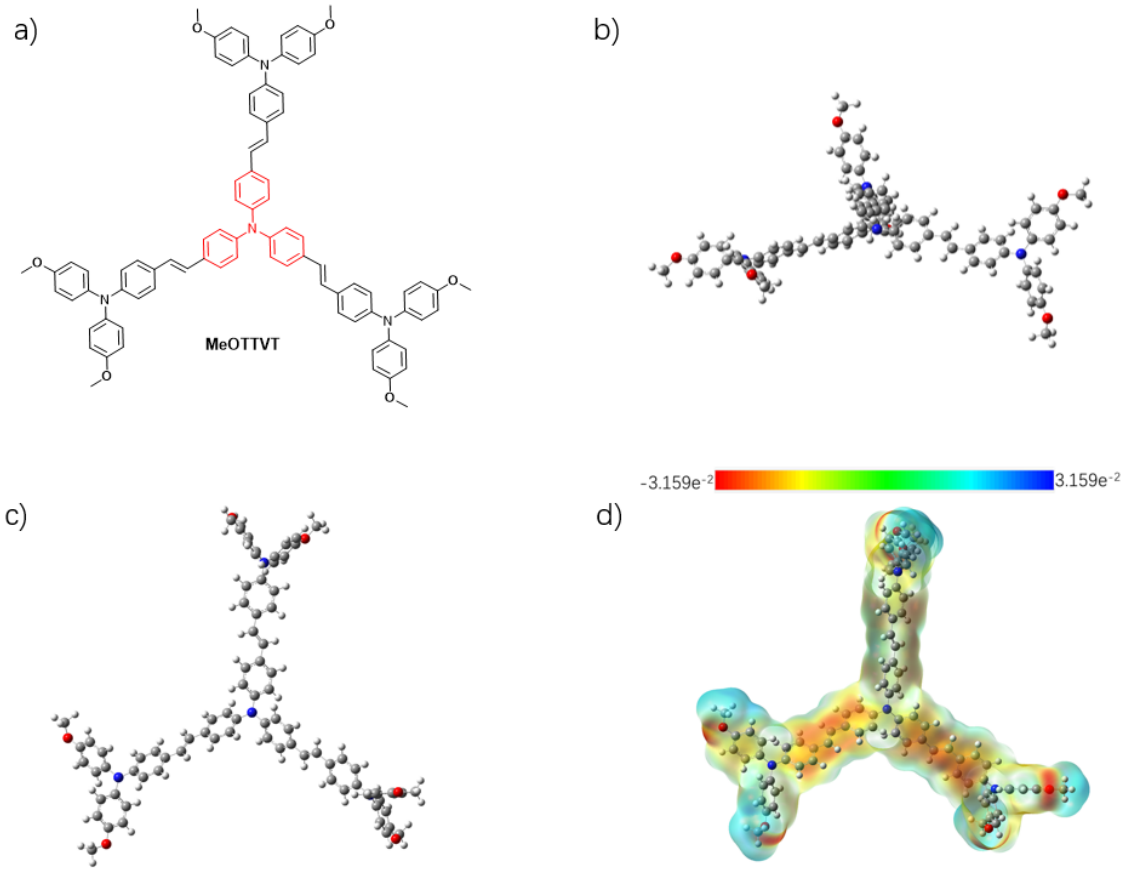

Figure 1. a) Structure of MeOTTVT. DFT calculation results of the MeOTTVT b) side view and c) top view of optimized ground-state molecular configurations. d) Electrostatic potential (ESP) surface of MeOTTVT.

The synthetic route to prepare MeOTTVT is depicted in **Scheme S1**. The synthesis starts from two steps of Vilsmeier-Haack reaction of triphenylamine, in which N,N-dimethylformamide and phosphorus oxychloride provide compound **1**. In the next step, a Wittig reaction of compound **1**, potassium tert-butoxide and diethyl (4-chlorobenzyl)phosphonate is employed to yield compound **2**. Subsequently, the Buchwald-Hartwig reaction of compound **2** and bis(4-methoxyphenyl)amine affords the final compounds MeOTTVT. All key intermediates and the final HTM were fully characterized by ^{1}**H** NMR, ^{13}**C** NMR and HR-MS spectrometry (**Figures S1-S9**). In order to estimate the real synthetic cost of the new HTM, we employ the total cost model that was described by Pablo et al.[43] and Tang et al.[44], most of the quotes being collected

from major chemical suppliers (such as Sigma-Aldrich, Alfa, TCI and Fischer) for corresponding chemicals used in the synthetic procedure of the MeOTTVT. Detailed synthetic cost evaluations are given in **Figures S10-S12** and **Tables S1-S3**. The estimated synthesis cost of compound MeOTTVT is calculated to be 34.28 $/g with a realistic overall production yield of 37.2%, which is considered a low-cost HTM in contrast with the mostly used *spiro*-OMeTAD and polytriarylamine (PTAA)[45].

Density functional theory (DFT) calculations at the B3LYP level is applied to investigate the molecular geometries, surface potential distribution, dipole moment and frontier orbital distribution of MeOTTVT[46]. As shown in **Figure 1b** and **1c**, the top and side view of the optimal molecular structure show that the molecule exhibits a pyramid shape with both partial planarity and quasi three-dimensionality properties, which is considered beneficial to increase π-π stacking in solid state while maintaining good solubility[47]. The smaller dipole moment of MeOTTVT (2.92 Debye) as compared to *spiro*-OMeTAD (5.8 Debye)[48] implies improved charge mobility for MeOTTVT[49]. As shown in **Figure S13**, the HOMO level of MeOTTVT is mainly distributed in the central and the lowest unoccupied molecular orbital (LUMO) on the methoxyl-substituted triphenylamine arms. Wang et al. report that spatially separated HOMO and LOMO levels is favorable to obtain good hole-mobility[50]. Electrostatic potential surface (EPS) of MeOTTVT was calculated (**Figure 1d**), showing that the negative charges are mainly concentrated on the methoxy group. Huang et al. also report that such electro-negativity of methoxyl substituted TPA can act as a Lewis base to passivate perovskite surface defect and increase the stability of PSCs[51].

Normalized UV-*vis* absorption spectrum of MeOTTVT, shown in **Figure 2a**, exhibits an absorption band at 415 nm and the characteristic absorption peak of triphenylamine at 300 nm. The optical band gap of MeOTTVT estimated from Tauc plot (inset of **Figure 2a**) is 2.74 eV. Cyclic voltammetry (CV) measurements of MeOTTVT using ferrocene as the reference (**Figure S14**) shows the HOMO level of MeOTTVT to be -5.24 eV against vacuum from the first oxidation wave. The LUMO level of MeOTTVT is calculated to be -2.50 eV by adding the band gap energy to the HOMO level. The energy diagram of perovskite photo-absorber and charge extraction layers are illustrated in **Figure 2b**. The valance band off-set between MeOTTVT and perovskite photo-absorber (-5.40 eV) generates a driving force of 0.16 eV for

the hole transfer from the perovskite to the HTL. Meanwhile, the deep HOMO energy level of -5.24 eV provides favorable band alignment with perovskite and thus reduces voltage loss.

Thermogravimetric analysis (TGA) and differential scanning calorimetry (DSC) was used to investigate the thermal stability of MeOTTVT and the corresponding HTL (**Figure S15)**. The thermal decomposition temperature (T_d) and glass transition temperature (T_g) are 373.96 ℃ and 137.06 ℃, respectively. The high T_g value guarantees morphology stability for MeOTTVT-based HTL, which is essential for the long-term photostability of PSCs[52-53].

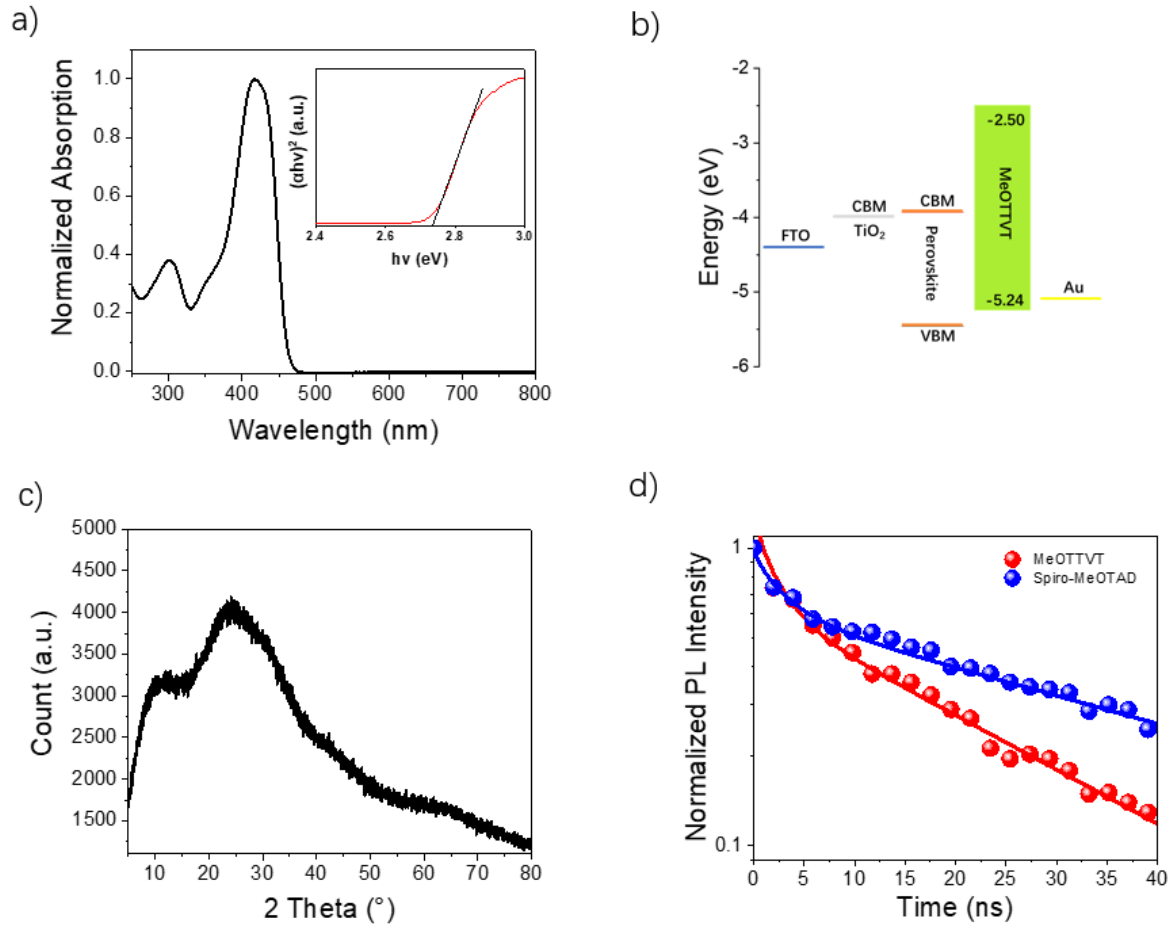

Figure 2. a) UV-vis spectrum of MeOTTVT thin film coated on glass with the inset showing Tauc plot. b) Energy level diagram for device components. c) X-ray diffraction (XRD) pattern of MeOTTVT thin film coated on glass substrate. d) TRPL of perovskite film coated with MeOTTVT and standard doped *spiro*-MeOTAD. The solid lines indicate the model fits.

Employing a partial planar structure geometry implies potential aggregation tendency for MeOTTVT, which is supported by X-ray diffraction (XRD) results of MeOTTVT thin film coated on glass substrate (**Figure 2c**). Although the thin film contained an amorphous phase

with no characteristic diffraction peaks, the broad feature in **Figure 2c** at around 25° indicates a π-π stacking between MeOTTVT molecules, which is important for increasing the hole mobility in the corresponding HTL[54]. We performed space-charge limited current (SCLC) measurements to derive the hole-mobility using a hole-only device with architecture of indium-doped tin oxide (ITO)/MoO_3 (10 nm)/MeOTTVT/MoO_3 (10 nm)/Al (80nm), and the results are shown in **Figure S16**. The SCLC hole-mobility of MeOTTVT is 4.62×10^{-4} cm^2V^{-1} s^{-1}, of the same order of magnitude compared to reported dopant additive free HTM[30, 54].

Time-resolved photoluminescence (TRPL) was performed to investigate the hole extraction ability at the perovskite/MeOTTVT interface. **Figure 2d** shows this measurement in comparison with the TRPL measurement for the perovskite/doped *spiro*-MeOTAD interface. Numerical simulations were applied to model the TRPL traces, the details of which have been described in our previous work[55]. Two different characteristics can be observed. The rapid decay within the first 10 ns is dominated by charge carrier diffusion after the initial laser-induced exponential carrier profile. After this an exponential decay is observed which comes mainly from hole transfer from the perovskite into the HTM. We modeled this with a charge carrier mobility of 1 cm^2/Vs and a hole extraction velocity of 700 cm/s for the perovskite/spiro-MeOTAD and 2500 cm/s for the perovskite/MeOTTVT interface. Note that this velocity could in principle also be interpreted as interface recombination, however, in our previous work we showed that this fast decay within the first 100 ns can be related to hole transfer[55]. These findings indicate a good hole-extraction ability of MeOTTVT. This can be attributed to the suitable HOMO level and the reduction of interfacial barriers.

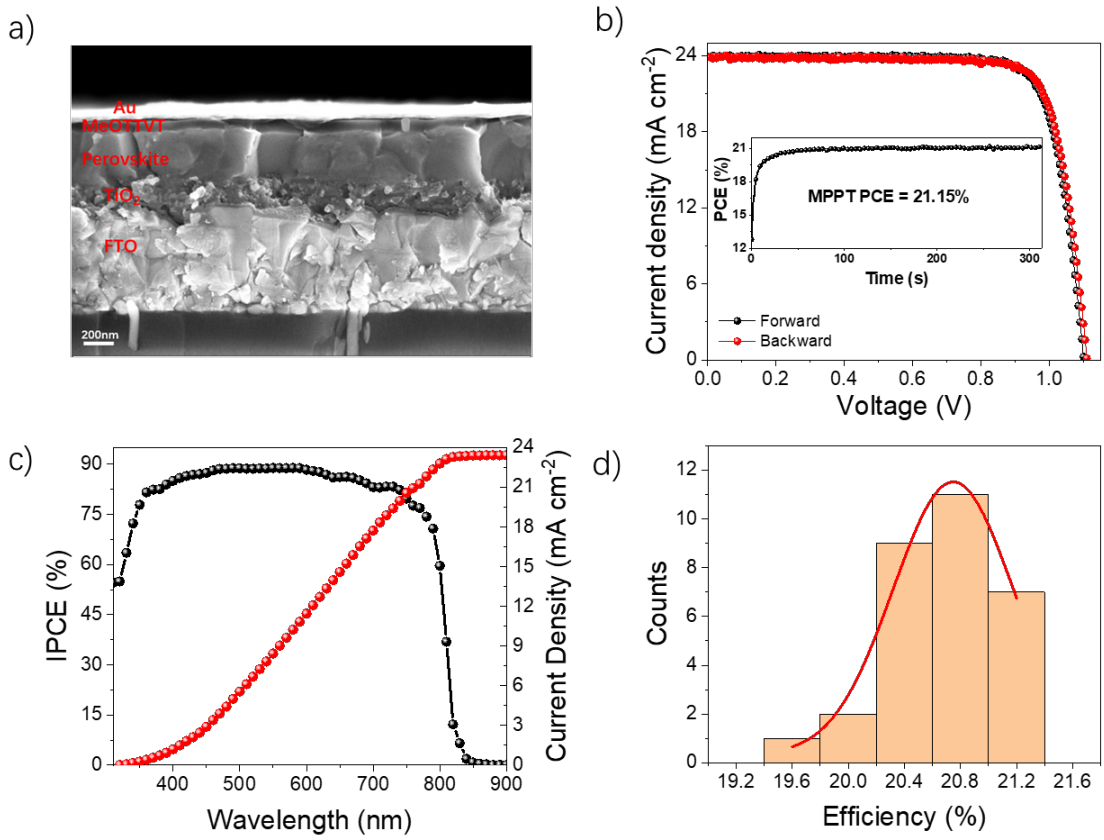

Figure 3. a) Cross-section scanning electron microscopy (SEM) photo of MeOTTVT based PSC. b) I–V curves of the champion PSC based dopant additive free MeOTTVT with the inset showing stable output of PSC device over 300s. c) IPCE of the device. d) Histogram of efficiencies from 30 individual devices based on MeOTTVT.

To prove the potential application of MeOTTVT in PSCs, we fabricated PSC devices with architecture of fluorine-doped tin oxide (FTO)/compact TiO_2/mesoscopic TiO_2/perovskite/HTL/gold, in which perovskite formulation $Cs_{0.05}FA_{0.85}MA_{0.10}Pb(I_{0.97}Br_{0.03})_3$ with 5% excess of PbI_2 was applied. The cross-sectional scanning electron microscopy (SEM) photo of a MeOTTVT based PSC is shown in **Figure 3a**. The optimized thickness of dopant additive free MeOTTVT HTL is estimated to be 40 nm. The Energy-level alignment of each component in perovskite solar cells is shown in **Figure 2b**. The current density–voltage (*J–V*) curves for one of our champion PSC under simulated 1-sun illumination is shown in **Figure 3b**, and the corresponding PV parameters are summarized in **Table 1**. The best-performing PSC based on MeOTTVT dopant additive free HTL shows an outstanding PCE of 21.30% with an open-circuit voltage (*V*oc) of 1111 mV, a short-circuit photocurrent (*J*sc) of 23.89 mA/cm^2 and a fill factor (FF) of 80.3%. Such a PCE sets a new benchmark for PSCs based on dopant additive free small molecule HTM. The lower hysteresis of 1.2% between the forward and reverse scan

for the MeOTTVT dopant-additive free HTL based PSC compare with doped *spiro*-OMeTAD based PSC (**Figure S17**) is attributed to eliminated ion movement, specifically Li^+ dopant in the control device[56-57]. The PCE statistics of 30 devices reflect good device reproducibility as shown in **Figure 3d**. The incident photon-to-electron conversion efficiency (IPCE) spectra of the champion devices is shown in **Figure 3c**. The integrated photocurrent is in good agreement with the measured *J*sc value (**Table 1**). The inset in **Figure 2b** shows power output at the maximum power point (MPP) for the best performing devices under dry ambient air (10% RH (relative humidity)) within 320 s (insert in **Figure 2b**). The MeOTTVT based PSC exhibits a stabilized PCE of 21.15%, which is consistent with the value derived the J-V curves.

Table 1. Photovoltaic parameters of champion PSC devices employing dopant additive free MeOTTVT-based HTL (measured under simulated AM 1.5G solar irradiance).

PSC	V_{OC} [V]	J_{SC}[c)] [mA/cm^2]	J_{SC}[d)] [mA/cm^2]	FF [%]	PCE[e)] [%]	PCE[f)] [%]
MeOTTVT RVS[a)]	1.111	23.89	23.42	80.3	21.30	21.17
MeOTTVT FWS[b)]	1.101	23.91		79.9	21.04	

a) reverse scan; b) forward scan; c) J_{SC} determined from the IV measurement; d) J_{SC} determined rom IPCE; e) PCE determined from the IV measurement; f) Average PCE of reverse and forward scan.

The stability of the PSCs based on dopant additive free MeOTTVT HTL under thermal stress and humid air is investigated, using devices based on doped *spiro*-OMeTAD as a reference. Shelf live data was obtained under ambient condition at a relative humidity (r.h.) of 40–60% without encapsulation, and the results are shown in **Figure 4a**. After 45 days the PCE of PSC based on dopant additive free MeOTTVT HTL decreased by less than 5%, while the PCE of standard (doped) *spiro*-OMeTAD based PSC decreased by ~50%. The superior stability of dopant additive-free MeOTTVT HTL based PSC can be attributed to two main reasons, *i*) larger contact angle of dopant additive free MeOTTVT compared to doped *spiro*-OMeTAD based HTL with water droplet shows reduced wetting by water for dopant additive free MeOTTVT based PSC as compared to *spiro*-OMeTAD. (**Figure S18**); *ii*) more stable perovskite/HTL interface for dopant additive free MeOTTVT HTL PSC as revealed by monitoring *V*oc and FF (**Figure 4c and 4d**) under simulated 1-sun illumination. Compared to doped *spiro*-OMeTAD-based device, the *V*oc and FF of dopant additive free MeOTTVT HTL based device remain

stable[55]. MeOTTVT HTL -based PSC stability under heat stress is measured holding the devices under 80 ℃ and monitor the PCE. (**Figure 4b)**. After 220 h, the PSC based on dopant additive free MeOTTVT HTL retained 90% of its initial efficiency, while the efficiency of spiro-OMeTAD-based device deceased by almost 70%. These results can be attributed to the higher T_g of MeOTTVT (T_g = 137.1 ℃) than that of doped spiro-OMeTAD (T_g ~ 75 ℃)[58].

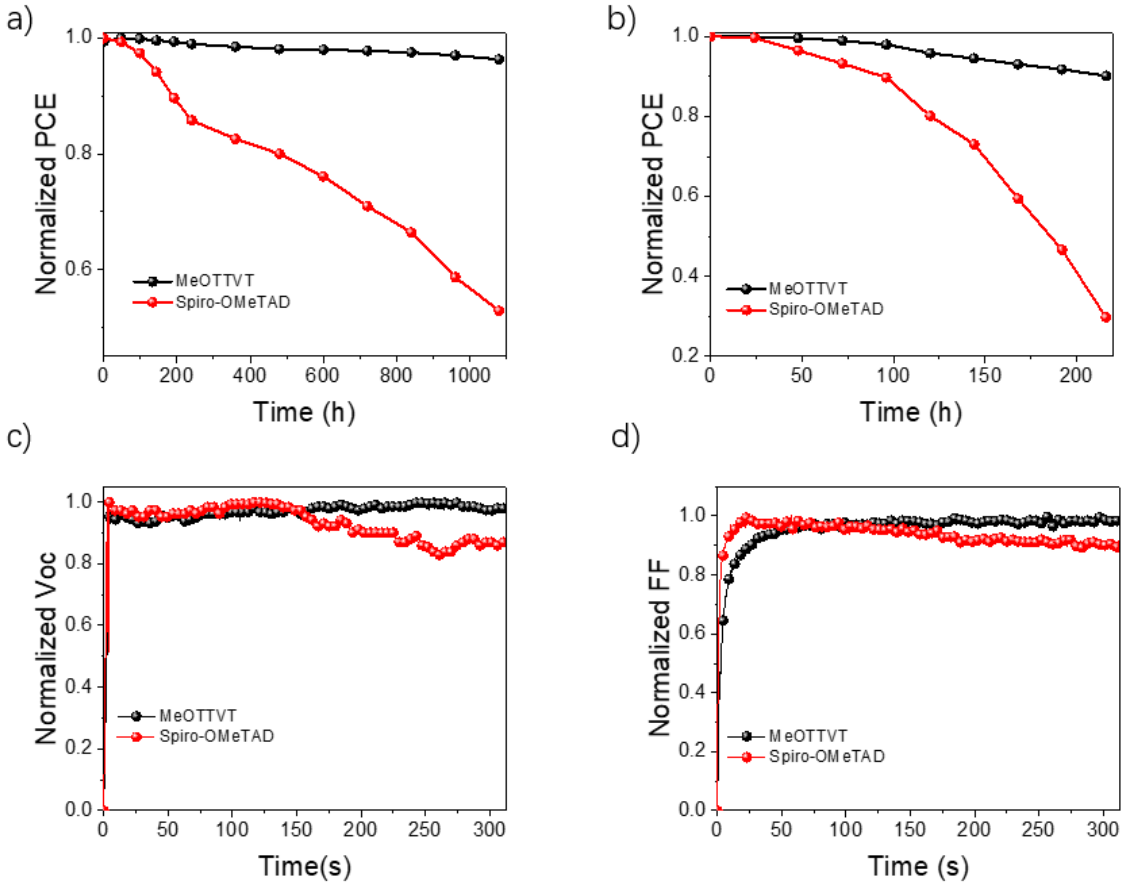

Figure 4. Device stabilities of PSCs with different HTMs under a) RH 40-60 % and b) 80℃ condition. c) *V*oc and d) FF of device based different HTMs change over time under 1 sun continuous illumination.

Conclusions

In conclusion, we conceived a novel pyramidal-shaped low-cost HTM, MeOTTVT and tested it for PSCs application. By judicious chemical designing, the quasi-pyramidal geometry endowed MeOTTVT π-π stacking tendency while maintaining appropriate solubility for processing. Sufficient hole-mobility that is related to the π-π stacking makes it possible for MeOTTVT finding its application as dopant additive free HTL. The three methoxyl triphenylamine arms provided suitable bandgap alignment with perovskite photoabsorber for

efficient hole-extraction. MeOTTVT provides a new benchmark PCE for dopant additive free small molecule HTL based PSC of 21.3% along with negligible hysteresis and good reproducibility. In addition, it also exhibits higher T_g and hydrophobicity as compared to *spiro*-OMeTAD. Dopant additive free MeOTTVT-based devices showed good stability against thermal stress and ambient moisture, retaining 96% of its initial PCE after 1100 h at RH 40-60% condition, and 90% of initial PCE after 220 h under 80 ℃. More importantly, the synthetic cost of MeOTTVT is only 34.28 $/g based on realistic production yield of 37.2%, potentially of low-cost for large throughput production in contrast with *spiro*-OMeTAD and PTAA. Our work opens a new pathway to design dopant additive free HTM promoting large scale applications of PSCs.

ASSOCIATED CONTENT

Supporting Information
Experimental section and additional characterization.

Acknowledgements
H.Z. thanks the China Scholarship Council for funding. Y.L., S.M.Z., and M.G. thank the King Abdulaziz City for Science and Technology (KACST) and the European Union's Horizon 2020 research and innovation program (grant agreement No 826013) for financial support. X.L. acknowledges the financial support from the National Science Foundation of China (No. 21676188). S.W. thanks the National Key Research and Development Program of China (2016YFB0401303). H.L. thanks the National Science Foundation for Young Scientists of China (No. 61804106). A.H. acknowledges the financial support from the Swiss National Science Foundation R'Equip program under the grant number 183305.

AUTHOR INFORMATION

Corresponding Author
*E-mail: zhongjin.shen@epfl.ch (Z.S.)
*E-mail: yuhang.liu@epfl.ch (Y.L.)
*E-mail: lixianggao@tju.edu.cn (X.L.)
*E-mail: michael.graetzel@epfl.ch (M.G.)

Author Contributions
H.Z. design and synthesized the HTM. Y.L. and M.G. conceived the idea of the work; H.Z. and Y.L. designed the project and fabricated and characterized devices; F.T.E. performed PL measurements; L.P. performed XRD and SEM measurement; Z.S. performed ^{1}H- and ^{13}C-NMR and HR-MS measurements and cost evaluation. J.H. performed DFT calculation. H.Z. wrote the manuscript; All the authors contributed toward finalizing the draft; S.M.Z. coordinated the project; M.G. and X.L. directed and supervised the research.

Notes
The authors declare no competing financial interest.

REFERENCE

1. Kojima, A.; Teshima, K.; Shirai, Y.; Miyasaka, T., Organometal Halide Perovskites as Visible-Light Sensitizers for Photovoltaic Cells. *J. Am. Chem. Soc.* **2009,** *131* (17), 6050-6051.
2. National Renewable Energy Laboratory Best Research-Cell Efficiency Chart. https://www.nrel.gov/pv/cell-efficiency.html.
3. Yu, D.; Hu, Y.; Shi, J.; Tang, H.; Zhang, W.; Meng, Q.; Han, H.; Ning, Z.; Tian, H., Stability improvement under high efficiency-next stage development of perovskite solar cells. *Sci. China: Chem.* **2019,** *62*, 684-707.
4. Liu, Y.; Akin, S.; Uchida, R.; Arora, N.; Milic, J. V.; Uhl, A. R.; Zakeeruddin, S. M.; Dar, M. I.; Gratzel, M.; Akin, S.; Pan, L.; Hagfeldt, A.; Uchida, R.; Hinderhofer, A.; Schreiber, F., Ultrahydrophobic 3D/2D fluoroarene bilayer-based water-resistant perovskite solar cells with efficiencies exceeding 22. *Sci. Adv.* **2019,** *5* (6), eaaw2543.
5. Yang, F.; Zhang, P.; Kamarudin, M. A.; Kapil, G.; Ma, T.; Hayase, S., Addition Effect of Pyreneammonium Iodide to Methylammonium Lead Halide Perovskite-2D/3D Heterostructured Perovskite with Enhanced Stability. *Adv. Funct. Mater.* **2018,** *28*, 1804856.
6. Ji, F.; Pang, S.; Zhang, L.; Zong, Y.; Cui, G.; Padture, N. P.; Zhou, Y., Simultaneous Evolution of Uniaxially Oriented Grains and Ultralow-Density Grain-Boundary Network in CH3NH3PbI3 Perovskite Thin Films Mediated by Precursor Phase Metastability. *ACS Energy Lett.* **2017,** *2* (12), 2727-2733.
7. Rong, Y.; Hu, Y.; Mei, A.; Tan, H.; Saidaminov, M. I.; Seok, S. I.; McGehee, M. D.; Sargent, E. H.; Han, H., Challenges for commercializing perovskite solar cells. *Science* **2018,** *361* (6408), eaat8235.
8. Long, M.; Zhang, T.; Chen, D.; Qin, M.; Chen, Z.; Gong, L.; Lu, X.; Xie, F.; Xie, W.; Chen, J.; Xu, J., Interlayer Interaction Enhancement in Ruddlesden-Popper Perovskite Solar Cells Towards High Efficiency and Phase Stability. *ACS Energy Lett.* **2019,** *4* (5), 1025-1033.
9. Zhang, F.; Kim, D. H.; Lu, H.; Park, J.-S.; Larson, B.; Hu, J.; Gao, L.; Xiao, C.; Reid, O.; Chen, X.; Zhao, Q.; Ndione, P. F.; Berry, J. J.; You, W.; Walsh, A.; Beard, M. C.; Zhu, K., Enhanced Charge Transport in 2D Perovskite via Fluorination of Organic Cation. *J. Am. Chem. Soc.* **2019,** *141*, 5972-5979.
10. Wu, G.; Li, X.; Zhou, J.; Zhang, J.; Zhang, X.; Leng, X.; Wang, P.; Chen, M.; Zhang, D.; Zhao, K.; Liu, S.; Zhou, H.; Zhang, Y., Fine Multi-Phase Alignments in 2D Perovskite Solar Cells with Efficiency over 17% via Slow Post-Annealing. *Adv. Mater.* **2019,** *31*, 1903889.
11. Lai, H.; Lu, D.; Xu, Z.; Zheng, N.; Xie, Z.; Liu, Y., Organic-Salt-Assisted Crystal Growth and Orientation of Quasi-2D Ruddlesden–Popper Perovskites for Solar Cells with Efficiency over 19%. *Adv. Mater.* **2020,** *30*, 2001470.
12. Qing, J.; Kuang, C.; Wang, H.; Wang, Y.; Liu, X.-K.; Bai, S.; Li, M.; Sum, T. C.; Hu, Z.; Zhang, W.; Gao, F., High-Quality Ruddlesden–Popper Perovskite Films Based on In Situ Formed Organic Spacer Cations. *Adv. Mater.* **2019,** *31* (41), 1904243.
13. Yu, S.; Liu, H.; Wang, S.; Zhu, H.; Dong, X.; Li, X., Hydrazinium cation mixed FAPbI3-based perovskite with 1D/3D hybrid dimension structure for efficient and stable solar cells. *Chem. Eng. J.* **2020,** *403*, 125724.
14. Wang, Y.; Wu, T.; Barbaud, J.; Kong, W.; Cui, D.; Chen, H.; Yang, X.; Han, L., Stabilizing heterostructures of soft perovskite semiconductors. *Science* **2019,** *365* (6454), 687-691.
15. Yang, S.; Chen, S.; Mosconi, E.; Fang, Y.; Xiao, X.; Wang, C.; Zhou, Y.; Yu, Z.; Zhao, J.; Gao, Y.; De Angelis, F.; Huang, J., Stabilizing halide perovskite surfaces for solar cell operation with wide-bandgap lead oxysalts. *Science* **2019,** *365* (6452), 473-478.
16. Li, H.; Shi, J.; Deng, J.; Chen, Z.; Li, Y.; Zhao, W.; Wu, J.; Wu, H.; Luo, Y.; Li, D.; Meng, Q., Intermolecular π-π Conjugation Self-Assembly to Stabilize Surface Passivation of

Highly Efficient Perovskite Solar Cells. *Adv. Mater.* **2020,** *32*, 1907396.
17. Zhang, F.; Yao, Z.; Guo, Y.; Li, Y.; Bergstrand, J.; Brett, C. J.; Cai, B.; Hajian, A.; Guo, Y.; Yang, X.; Gardner, J. M.; Widengren, J.; Roth, S. V.; Kloo, L.; Sun, L., Polymeric, Cost-Effective, Dopant-Free, Hole Transport Materials for Efficient and Stable Perovskite Solar Cells. *J. Am. Chem. Soc.* **2019,** *141*, 19700-19707.
18. Kou, C.; Feng, S.; Li, H.; Li, W.; Li, D.; Meng, Q.; Bo, Z., A Molecular "Flower" as the High Mobility Hole Transport Material for Perovskite Solar Cells. *ACS Appl. Mater. Interfaces* **2017,** *9* (50), 43855-43860.
19. Peckus, D.; Matulaitis, T.; Franckevičius, M.; Mimaitė, V.; Tamulevičius, T.; Simokaitienė, J. r.; Volyniuk, D.; Gulbinas, V.; Tamulevičius, S.; Gražulevičius, J. V., Twisted Intramolecular Charge Transfer States in Trinary Star-Shaped Triphenylamine-Based Compounds. *J. Phys. Chem. A* **2018,** *122* (12), 3218-3226.
20. Pham, H. D.; Yang, T. C.-J.; Jain, S. M.; Wilson, G. J.; Sonar, P., Development of Dopant-Free Organic Hole Transporting Materials for Perovskite Solar Cells. *Adv. Energy Mater.* **2020,** *10*, 1903326.
21. Min, H.; Kim, M.; Lee, S.-U.; Kim, H.; Kim, G.; Choi, K.; Lee, J. H.; Seok, S. I., Efficient, stable solar cells by using inherent bandgap of α-phase formamidinium lead iodide. *Science* **2019,** *366* (6466), 749-753.
22. Liu, X.; Zhang, F.; Liu, Z.; Xiao, Y.; Wang, S.; Li, X., Dopant-free and low-cost molecular "bee" hole-transporting materials for efficient and stable perovskite solar cells. *J. Mater. Chem. C* **2017,** *5* (44), 11429-11435.
23. Schloemer, T. H.; Gehan, T. S.; Christians, J. A.; Mitchell, D. G.; Dixon, A.; Li, Z.; Zhu, K.; Berry, J. J.; Luther, J. M.; Sellinger, A., Thermally Stable Perovskite Solar Cells by Systematic Molecular Design of the Hole-Transport Layer. *ACS Energy Lett.* **2019,** *4* (2), 473-482.
24. Pham, H. D.; Jain, S. M.; Li, M.; Wang, Z.-K.; Manzhos, S.; Feron, K.; Pitchaimuthu, S.; Liu, Z.; Motta, N.; Durrant, J. R.; Sonar, P., All-Rounder Low-Cost Dopant-Free D-A-D Hole-Transporting Materials for Efficient Indoor and Outdoor Performance of Perovskite Solar Cells. *Adv. Electron. Mater.* **2020,** *6*, 1900884.
25. Zhang, F.; Liu, X.; Yi, C.; Bi, D.; Luo, J.; Wang, S.; Li, X.; Xiao, Y.; Zakeeruddin, S. M.; Grätzel, M., Dopant-Free Donor (D)–π–D–π–D Conjugated Hole-Transport Materials for Efficient and Stable Perovskite Solar Cells. *ChemSusChem* **2016,** *9*, 2578-2585.
26. Habisreutinger, S. N.; Wenger, B.; Snaith, H. J.; Nicholas, R. J., Dopant-Free Planar n-i-p Perovskite Solar Cells with Steady-State Efficiencies Exceeding 18%. *ACS Energy Lett.* **2017,** *2* (3), 622-628.
27. Zhang, W.; Wan, L.; Li, X.; Wu, Y.; Fu, S.; Fang, J., A dopant-free polyelectrolyte hole-transport layer for high efficiency and stable planar perovskite solar cells. *J. Mater. Chem. A* **2019,** *7*, 18898-18905.
28. Zhang, J.; Zhang, T.; Jiang, L.; Bach, U.; Cheng, Y.-B., 4-tert-Butylpyridine Free Hole Transport Materials for Efficient Perovskite Solar Cells: A New Strategy to Enhance the Environmental and Thermal Stability. *ACS Energy Lett.* **2018,** *3* (7), 1677-1682.
29. Xiao, C.; Zhang, F.; Li, Z.; Harvey, S. P.; Chen, X.; Wang, K.; Jiang, C.-S.; Zhu, K.; Al-Jassim, M., Inhomogeneous Doping of Perovskite Materials by Dopants from Hole-Transport Layer. *Matter* **2020,** *2* (1), 261-272.
30. Yin, C.; Lu, J.; Xu, Y.; Yun, Y.; Wang, K.; Li, J.; Jiang, L.; Sun, J.; Scully, A. D.; Huang, F.; Zhong, J.; Wang, J.; Cheng, Y.-B.; Qin, T.; Huang, W., Low-Cost N,N'-Bicarbazole-Based Dopant-Free Hole-Transporting Materials for Large-Area Perovskite Solar Cells. *Adv. Energy Mater.* **2018,** *8*, 1800538.
31. Han, D.; Wu, C.; Zhang, Q.; Wei, S.; Qi, X.; Zhao, Y.; Chen, Y.; Chen, Y.; Xiao, L.; Zhao, Z., Solution-Processed Cu9S5 as a Hole Transport Layer for Efficient and Stable

Perovskite Solar Cells. *ACS Appl. Mater. Interfaces* **2018,** *10* (37), 31535-31540.
32. Akin, S.; Liu, Y.; Dar, M. I.; Zakeeruddin, S. M.; Gratzel, M.; Turan, S.; Sonmezoglu, S., Hydrothermally processed CuCrO2 nanoparticles as an inorganic hole transporting material for low-cost perovskite solar cells with superior stability. *J. Mater. Chem. A* **2018,** *6*, 20327-20337.
33. Jung, E. H.; Jeon, N. J.; Park, E. Y.; Moon, C. S.; Yang, T.-Y.; Noh, J. H.; Seo, J.; Moon, C. S.; Noh, J. H.; Shin, T. J., Efficient, stable and scalable perovskite solar cells using poly(3-hexylthiophene). *Nature* **2019,** *567* (7749), 511-515.
34. Rezaee, E.; Liu, X.; Hu, Q.; Dong, L.; Chen, Q.; Pan, J.-H.; Xu, Z.-X., Dopant-Free Hole Transporting Materials for Perovskite Solar Cells. *Sol. RRL* **2018,** *2* (11), 1800200.
35. Kazim, S.; Ramos, F. J.; Gao, P.; Nazeeruddin, M. K.; Grätzel, M.; Ahmad, S., A dopant free linear acene derivative as a hole transport material for perovskite pigmented solar cells. *Energy Environ. Sci.* **2015,** *8* (6), 1816-1823.
36. Zhou, W.; Wen, Z.; Gao, P., Less is More: Dopant-Free Hole Transporting Materials for High-Efficiency Perovskite Solar Cells. *Adv. Energy Mater.* **2018,** *8*, 1702512.
37. Shen, C.; Wu, Y.; Zhang, H.; Li, E.; Zhang, W.; Xu, X.; Wu, W.; Tian, H.; Zhu, W., Semi-Locked Tetrathienylethene as Promising Building Block for Hole Transporting Materials: Toward Efficient and Stable Perovskite Solar Cells. *Angew. Chem., Int. Ed.* **2019,** *58*, 3784-3789.
38. Cao, Y.; Li, Y.; Morrissey, T.; Lam, B.; Patrick, B. O.; Dvorak, D. J.; Xia, Z.; Kelly, T. L.; Berlinguette, C. P., Dopant-free molecular hole transport material that mediates a 20% power conversion efficiency in a perovskite solar cell. *Energy Environ. Sci.* **2019,** *12*, 3502-3507.
39. Zhang, F.; Yi, C.; Wei, P.; Bi, X.; Luo, J.; Jacopin, G.; Wang, S.; Li, X.; Xiao, Y.; Zakeeruddin, S. M.; Grätzel, M., A Novel Dopant-Free Triphenylamine Based Molecular "Butterfly" Hole-Transport Material for Highly Efficient and Stable Perovskite Solar Cells. *Adv. Energy Mater.* **2016,** *6*, 1600401.
40. Pham, H. D.; Do, T. T.; Kim, J.; Charbonneau, C.; Manzhos, S.; Feron, K.; Tsoi, W. C.; Durrant, J. R.; Jain, S. M.; Sonar, P., Molecular Engineering Using an Anthanthrone Dye for Low-Cost Hole Transport Materials: A Strategy for Dopant-Free, High-Efficiency, and Stable Perovskite Solar Cells. *Adv. Energy Mater.* **2018,** *8*, 1703007.
41. Wang, Y.; Chen, W.; Wang, L.; Tu, B.; Chen, T.; Liu, B.; Yang, K.; Koh, C. W.; Zhang, X.; Sun, H.; Chen, G.; Feng, X.; Woo, H. Y.; Djurisic, A. B.; He, Z.; Guo, X., Dopant-Free Small-Molecule Hole-Transporting Material for Inverted Perovskite Solar Cells with Efficiency Exceeding 21%. *Adv. Mater.* **2019,** *31*, 1902781.
42. Saliba, M.; Orlandi, S.; Matsui, T.; Aghazada, S.; Cavazzini, M.; Correa-Baena, J.-P.; Gao, P.; Scopelliti, R.; Mosconi, E.; Dahmen, K.-H.; De Angelis, F.; Abate, A.; Hagfeldt, A.; Pozzi, G.; Graetzel, M.; Nazeeruddin, M. K., A molecularly engineered hole-transporting material for efficient perovskite solar cells. *Nat. Energy* **2016,** *1* (2), 15017.
43. Petrus, M. L.; Bein, T.; Dingemans, T. J.; Docampo, P., A low cost azomethine-based hole transporting material for perovskite photovoltaics. *J. Mater. Chem. A* **2015,** *3* (23), 12159-12162.
44. Zhou, J.; Yin, X.; Dong, Z.; Ali, A.; Song, Z.; Shrestha, N.; Bista, S. S.; Bao, Q.; Ellingson, R. J.; Yan, Y.; Tang, W., Dithieno[3,2-b:2',3'-d]pyrrole Cored p-Type Semiconductors Enabling 20 % Efficiency Dopant-Free Perovskite Solar Cells. *Angew. Chem., Int. Ed.* **2019,** *58*, 13717-13721.
45. Merck,https://www.sigmaaldrich.com/.
46. Dong, Y.; Zhu, H.; Cao, X.; Han, Y.-P.; Zhang, H.-Y.; Yang, Q.; Zhang, Y.; Zhao, J.; Yin, G.; Wang, S., Simple 9,10-Dihydrophenanthrene Based Hole-Transporting Materials for Efficient Perovskite Solar Cells. *Chem. Eng. J.* **2020,** *402*, 126298.

47. You, G.; Zhuang, Q.; Wang, L.; Lin, X.; Zou, D.; Lin, Z.; Zhen, H.; Zhuang, W.; Ling, Q., Dopant-Free, Donor-Acceptor-Type Polymeric Hole-Transporting Materials for the Perovskite Solar Cells with Power Conversion Efficiencies over 20%. *Adv. Energy Mater.* **2020,** *10*, 1903146.
48. Li, Y.; Li, H.; Zhong, C.; Sini, G.; Bredas, J.-L., Characterization of intrinsic hole transport in single-crystal spiro-OMeTAD. *npj Flexible Electron.* **2017,** *1* (1), 1-8.
49. Friederich, P.; Meded, V.; Poschlad, A.; Neumann, T.; Rodin, V.; Stehr, V.; Symalla, F.; Danilov, D.; Lüdemann, G.; Fink, R. F.; Kondov, I.; von Wrochem, F.; Wenzel, W., Molecular Origin of the Charge Carrier Mobility in Small Molecule Organic Semiconductors. *Adv. Funct. Mater.* **2016,** *26* (31), 5757-5763.
50. Wang, L.; Zhang, J.; Liu, P.; Xu, B.; Zhang, B.; Chen, H.; Inge, A. K.; Li, Y.; Wang, H.; Cheng, Y.-B.; Kloo, L.; Sun, L., Design and synthesis of dopant-free organic hole-transport materials for perovskite solar cells. *Chem. Commun.* **2018,** *54*, 9547-9692.
51. Huang, C.; Fu, W.; Li, C.-Z.; Zhang, Z.; Qiu, W.; Shi, M.; Heremans, P.; Jen, A. K. Y.; Chen, H., Dopant-Free Hole-Transporting Material with a C3h Symmetrical Truxene Core for Highly Efficient Perovskite Solar Cells. *J. Am. Chem. Soc.* **2016,** *138* (8), 2528-2531.
52. Tang, W.; Dong, Z.; Yin, X.; Ali, A.; Zhou, J.; Bista, S. S.; Chen, C.; Yan, Y., A Dithieno[3,2-b:2',3'-d]pyrrole Cored Four-Arm Hole Transporting Material Enables Over 19% Efficiency Dopant-Free Perovskite Solar Cells. *J. Mater. Chem. C* **2019,** *7*, 9455-9459.
53. Kong, X.; Jiang, Y.; Wu, X.; Chen, C.; Guo, J.; Liu, S.; Gao, X.; Zhou, G.; Liu, J.-M.; Kempa, K.; Gao, J., Dopant-free F-substituted benzodithiophene copolymer hole-transporting materials for efficient and stable perovskite solar cells. *J. Mater. Chem. A* **2020,** *8*, 1858-1684.
54. Paek, S.; Qin, P.; Lee, Y.; Cho, K. T.; Gao, P.; Grancini, G.; Oveisi, E.; Gratia, P.; Rakstys, K.; Al-Muhtaseb, S. A.; Ludwig, C.; Ko, J.; Nazeeruddin, M. K., Dopant-Free Hole-Transporting Materials for Stable and Efficient Perovskite Solar Cells. *Adv. Mater.* **2017,** *29* (35), 1606555.
55. Zhu, H.; Liu, Y.; Eickemeyer, F. T.; Pan, L.; Ren, D.; Ruiz-Preciado, M. A.; Carlsen, B.; Yang, B.; Dong, X.; Wang, Z.; Liu, H.; Wang, S.; Zakeeruddin, S. M.; Hagfeldt, A.; Dar, M. I.; Li, X.; Grätzel, M., Tailored Amphiphilic Molecular Mitigators for Stable Perovskite Solar Cells with 23.5% Efficiency. *Adv. Mater.* **2020,** *32*, 1907757.
56. Zhu, H.; Zhang, F.; Xiao, Y.; Wang, S.; Li, X., Suppressing defects through thiadiazole derivatives that modulate CH3NH3PbI3 crystal growth for highly stable perovskite solar cells under dark conditions. *J. Mater. Chem. A* **2018,** *6*, 4971-4980.
57. Liu, P.; Wang, W.; Liu, S.; Yang, H.; Shao, Z., Fundamental Understanding of Photocurrent Hysteresis in Perovskite Solar Cells. *Adv. Energy Mater.* **2019,** *9*, 1803017.
58. Jeon, N. J.; Na, H.; Jung, E. H.; Yang, T.-Y.; Lee, Y. G.; Kim, G.; Shin, H.-W.; Il Seok, S.; Lee, J.; Seo, J., A fluorene-terminated hole-transporting material for highly efficient and stable perovskite solar cells. *Nat. Energy* **2018,** *3*, 682-689.